Materials Science and Engineering A 550 (2012) 76–79

Contents lists available at SciVerse ScienceDirect

Materials Science and Engineering A

journal homepage: www.elsevier.com/locate/msea

Mechanical performance of $LaCrO_3$ doped with strontium and cobalt for SOFC interconnect

W. Acchar[a,*], C.R.C. Sousa[a], S.R.H. Mello-Castanho[b]

[a] Post-Graduation Program of Science and Materials Engineering, Federal University of Rio Grande do Norte (UFRN), CEP 59072-970, Brazil
[b] Intituto de Pesquisas Energéticas e Nucleares-IPEN/CNEN, Brazil

ARTICLE INFO

Article history:
Received 18 February 2012
Received in revised form 2 April 2012
Accepted 3 April 2012
Available online 15 April 2012

Keywords:
Lanthanum chromite
Sintering
Strength
Hardness

ABSTRACT

Doped lanthanum chromite was investigated as ceramic interconnect materials to be used in high-temperature solid oxide fuel cells (SOFCs). In this work, a $La_{0.80}Sr_{0.20}Cr_{0.92}Co_{0.08}O_3$ powder produced by combustion synthesis was used to obtain dense specimens. Powders were uniaxially compacted under a load of 30 MPa and sintered at 1500 °C for 4 h in air. The sintered specimens were characterized in terms of crystalline phases, density and porosity, strength and hardness measurements, deformation behavior, fracture mode and microstructure aspects. The results have shown dense samples (6.09 g/cm^3) with strength and hardness values of 62 MPa and 5.98 GPa, respectively. Surface micrograph indicates a mixture of inter- and transgranular fracture modes, a brittle deformation behavior and grain size around 3 μm.

1. Introduction

Solid oxide fuel cells (SOFCs) represent the most efficient way to generate electricity by electrochemical reaction between fuel and oxygen [1–7]. An SOFC consists mainly of an anode, a cathode and an electrolyte. A SOFC requires an interconnect material to form a SOFC stack and to make the electrical connection between the anode and the cathode [8–10]. The most important role of the interconnect materials is to provide a conductive path for electrical current and they have some characteristics such as good electrical conductivity to minimize ohmic losses, stability in both oxidizing and reducing conditions, similar thermal expansion coefficient (close to the other cell components) to minimize thermal stresses and to avoid the formation of cracks, chemical compatibility with the other cell components, mechanical properties at room and 900–1000 °C (operating cell temperature), low permeability to oxygen and hydrogen and low cost. Lanthanum chromite ($LaCrO_3$) is the most used interconnector material in solid oxide fuel cells (SOFCs) [11–17]. The main disadvantage of the lanthanum chromite is the high melting point and its difficulty to obtain fully densified products. Several studies have been developed in order to obtain dense optimize $LaCrO_3$ products and to optimize the physical and mechanical properties of doped $LaCrO_3$. Hydrothermal synthesis of doped lanthanum chromite [6,16], autoignition process [7], ultrasonic spray pyrolysis and glycine nitrate [9], slip casting [11], combustion process [11,17] and the incorporation of a variety of elements such as Ca (improving the sintering process and the conductivity values) [1,7,15], Ca—Co (increasing the strength values) [12], Sr (increasing densification) [14,16], Sr—Co—Fe (showing the presence of a ferrous-elastic behavior) [13] and the addition of glass material (improving the sinterability) [15] were reported. Further studies are still under way to identify the best combination of best elements to improve the density, conductivity and mechanical properties of lanthanum chromite. In addition, it was recently found that Sr—Co doped powders have good sinterability in air atmosphere and relative densities over the range of 93–96% may be achieved at temperature as low as 1600 °C [17]. Although the sinterability of the $La_{0.8}Sr_{0.20}Cr_{0.92}Co_{0.08}O_3$ interconnect material has been studied, the mechanical properties of the sintered material have still not been investigated in detail.

The main purpose of this study is to provide data on the facture strength and deformation behavior of $La_{0.8}Sr_{0.20}Cr_{0.92}Co_{0.08}O_3$.

2. Experimental procedure

Powder with expected stoichiometry $La_{0.80}Sr_{0.20}Cr_{0.92}Co_{0.08}O_3$ was prepared by combustion synthesis in laboratory. Combustion synthesis has allowed obtaining $La_{0.80}Sr_{0.20}Cr_{0.92}Co_{0.08}O_3$ perovskite powder from the corresponding metal nitrates and urea as fuel. Details about the powder process can be founded elsewhere [17]. Powder compacts were uniaxially pressed under 30 MPa and sintered at 1500 °C for 4 h in air. Apparent density and porosity of the sintered bodies were determined using the Archimedes water displacement method. Crystalline phases present after the

* Corresponding author. Tel.: +55 8432153793; fax: +55 8432153791.
E-mail address: acchar@dfte.ufrn.br (W. Acchar).

0921-5093/$ – see front matter © 2012 Elsevier B.V. All rights reserved.
http://dx.doi.org/10.1016/j.msea.2012.04.026

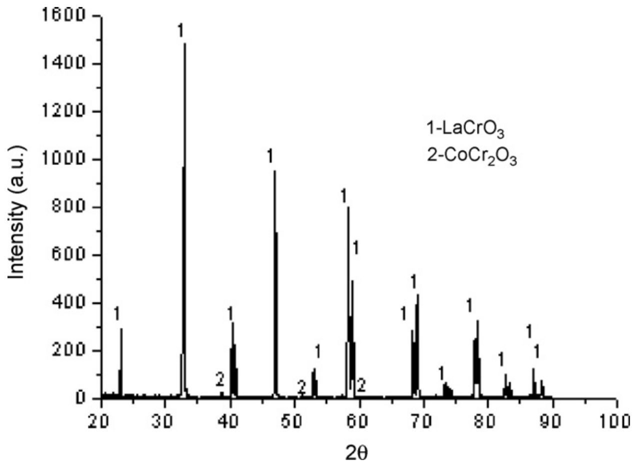

Fig. 1. X-ray diffraction pattern of sintered $La_{0.8}Sr_{0.20}Cr_{0.92}Co_{0.08}O_3$.

sintering process were identified by X-ray diffraction (Shimadzu XRD-600) in a range of 20–90° with a 2θ scanning rate of 2° min^{-1}. Vickers's microhardness (H_V) was evaluated by a Vickers indenter applying a load of 90 N during 15 s. Mechanical strength of the specimens (average of samples per value) was measured at ambient temperature and 900 °C by a universal testing machine (Zwick, 2.5 kN), using three-point bending geometry at a constant cross-head speed of 0.5 mm min^{-1}. Fracture surfaces were observed through by scanning electron microscopy (Shimadzu SSX-550).

3. Results and discussion

Fig. 1 depicts a typical X-ray diffraction pattern of the sintered $La_{0.8}Sr_{0.20}Cr_{0.92}Co_{0.08}O_3$ material. $LaCrO_3$ and $CoCr_2O_4$ with orthorhombic perovskite phase are shown to be the only crystalline phases present. No other secondary crystalline phases were identified. This corroborates findings reported in the literature for $LaCrO_3$ doped with strontium and cobalt [17,18]. There are other crystalline phases reported in the literature for $LaCrO_3$ based ceramic doped with Co ($LaCoO_3$) [12], Ca ($La_{0.8}Ca_{0.2}CrO_3$) [15], Sr ($La_{0.9}Sr_{0.1}CrO_3$) [16], Ca–Co ($La_{1-x}Ca_xCr_{1-y}O_{3-\delta}$) [3], Sr–Co ($La_{0.7}Sr_{0.3}Cr_{1-y}Co_yO_3$) [14] and Ca–M (M = Al, Co, Cu, Fe) ($(La_{0.8}Ca_{0.2}Cr_{0.9}M_{0.1})_{3-\delta}$ [1].

Table 1 summarizes some properties of lanthanum chromite investigated in this work. The density and porosity values obtained are comparable to those described in the literature [1,10,12,14,16]. Density values of $La_{1-x}Sr_xCr_{1-y}Co_yO_3$ materials sintered at 1500 °C were founded to increase with increasing strontium content and reached an ideal value at $x = 0.1$ and $y = 0.2$ or $x = 0.1$ and $y = 0.3$ [14]. Further increase in the dopant concentration, however, did not show to enhance the density values of lanthanum chromite materials [14]. Recent work published in the literature indicates the use of glass to improve the sintering process of lanthanum chromite [15]. The addition of glass increases the sintering ability, improving the densities values and the electrical conductivity [15].

Table 1
Properties of sintered $La_{0.80}Sr_{0.20}Cr_{0.92}Co_{0.08}O_3$.

	ρ [g/cm^3]	P [%]	H_V [GPa]	σ [MPa]
$La_{0.80}Sr_{0.20}Cr_{0.92}Co_{0.08}O_3$	6.09	0.7	5.98	62

Fig. 2 compares the strength and hardness values founded in this work with data reported in the literature for other lanthanum chromite materials [1,12]. Some studies published in the literature indicated that strength and hardness values are dependent on the porosity of the lanthanum chromite materials [10,12,14]. $LaSrCoO_3$ with 10% of porosity and dense samples of $LaCaCoO_3$ show hardness values between 7 and 9 GPa and 9 and 11 GPa, respectively [12]. Dense $La_{0.8}Ca_{0.2}CoO_3$ (99% TD) has a bending strength of 150 MPa whereas the more porous $LaCoO_3$ (83% TD) and $La_{0.8}Sr_{0.2}CoO_3$ (90% TD) have lower values of 53, 76 and 150 MPa, respectively [12]. Strength values of lanthanum chromite doped with strontium shows values of 130 and 180 MPa for sintering temperature of 1500 and 1700 °C [10,14]. The values of hardness and strength founded are compatible with the sintering temperature used in this work (1500 °C) and the observed porosity of 0.7% (Table 1).

Typical load–displacement curves measured at room- and high temperatures are shown in Fig. 3. Both curves show a linear behavior. The strength and deformation behavior of the interconnect material may be well matched with the other elements of the solid fuel cell. No similar deformation with the other cell elements and low high temperature strength can cause a collapse of the cell. $LaCrO_3$ doped with Fe have showed a ferrous-elastic behavior and a non-linear load–displacement behavior between room temperature and 700 °C [13]. This result is associated to the ferrous-elastic of the rhombohedral phase that not exists in the high temperature cubic symmetry [13].

An unusual deformation behavior was observed for lanthanum strontium manganese (LSM) [9]. Plastic deformation of LSM under ambient conditions under a bending stress of 40 MPa or less was

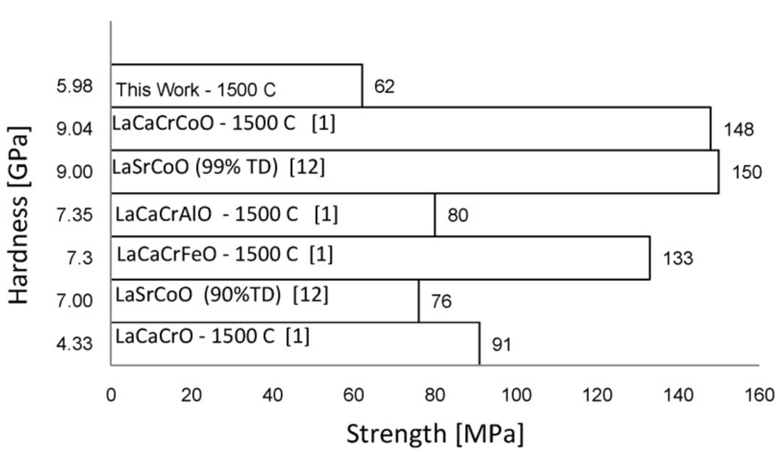

Fig. 2. Strength and hardness values of some lanthanum chromite materials.

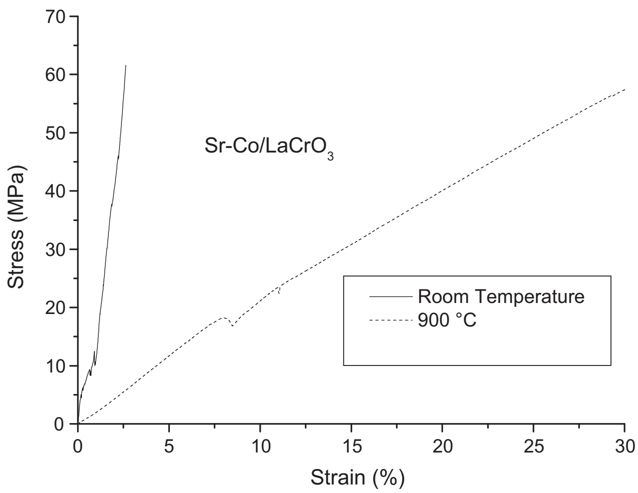

Fig. 3. Load–displacement curve of $La_{0.8}Sr_{0.20}Cr_{0.92}Co_{0.08}O_3$ at room temperature and 900 °C.

reported [9]. In this work no anomalous plastic deformation at ambient temperature was founded for $LaCrO_3$ doped with strontium and cobalt.

At 900 °C a decrease of the slope is observed and may be attributed to the decrease of elastic moduli of lanthanum chromite at high temperatures. A decrease of strength values of the sintered $La_{1-x}Sr_xCr_{1-y}Co_yO_3$ material with increasing temperature was also observed [14], which is in agreement with the results of Fig. 3.

Figs. 4–6 show the typical microstructure of the sintered $LaCrO_3$ sintered at 1500 °C. The $LaCrO_3$ material doped with strontium and cobalt samples exhibited a dense microstructure formed by equiaxed grains, but some residual porosity was also observed (Fig. 4). The microstructure consists of fine grains with an average size of approximately 3 μm (Figs. 4 and 5).

The fracture surface analysis reveals a mixture of transgranular and intergranular fracture modes (Fig. 5) what is in agreement with the fracture analysis observed for porous $LaCrO_3$ [12]. However, pores in triple point junction of approximately 2–4 μm diameters were also present (Fig. 6), which are possibly the sources of failure

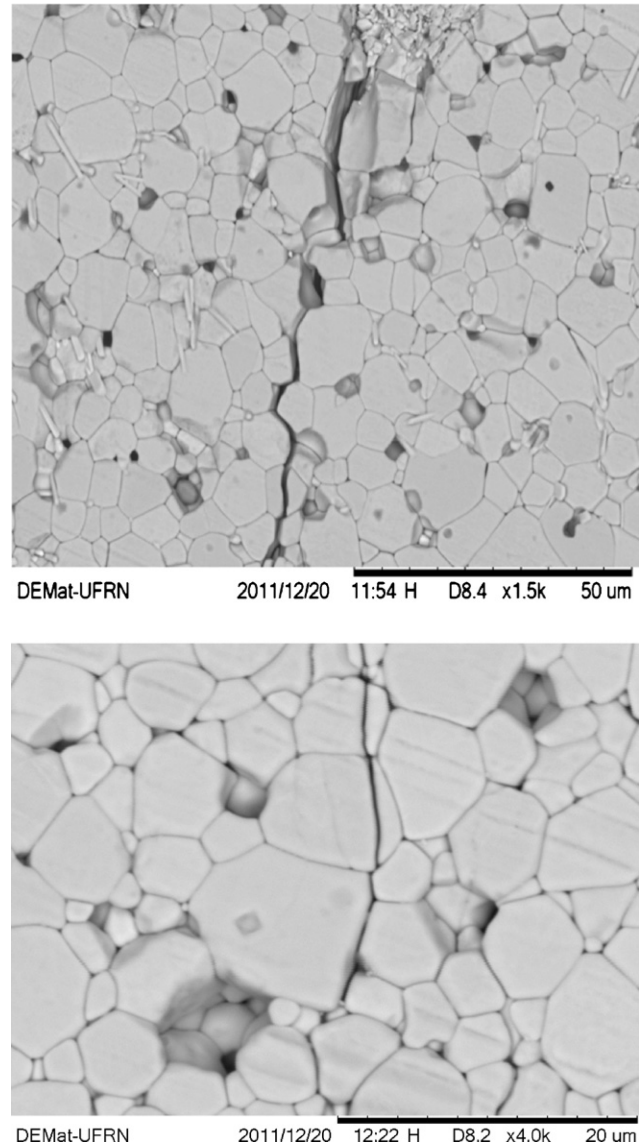

Fig. 5. SEM micrograph showing the crack propagation in $LaCrO_3$ grains.

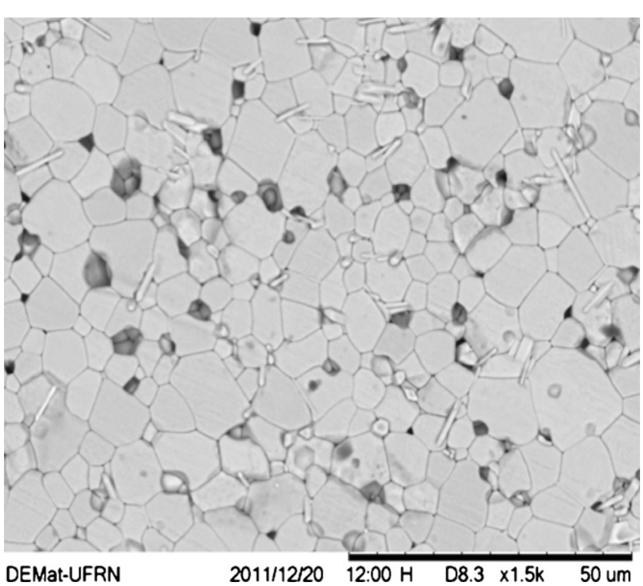

Fig. 4. SEM micrograph of the sintered material.

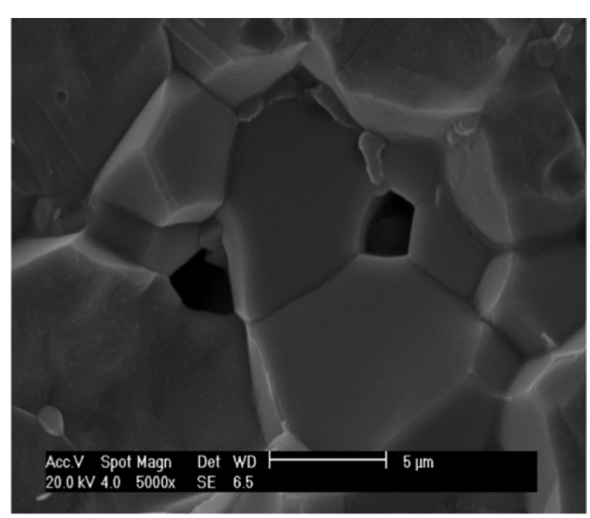

Fig. 6. Fracture surface of $La_{0.8}Sr_{0.20}Cr_{0.92}Co_{0.08}O_3$.

for these materials. These observations are in accordance with the density of lanthanum chromite presented in Table 1.

4. Conclusions

$La_{0.80}Sr_{0.20}Cr_{0.92}Co_{0.08}O_3$ powder prepared by combustion synthesis was used to sinter specimens at 1500 °C for 4 h. $LaCrO_3$ and $CoCr_2O_4$ with orthorhombic perovskite phase are the phases identified by X-ray diffraction. The lanthanum chromite material shows a density and porosity values of 6.09 g/cm^3 and 0.7%, respectively. The $LaCrO_3$ doped with strontium and cobalt shows strength (62 MPa) and hardness (5.98 GPa) comparable to other lanthanum chromite materials. Microstructural analyses have shown a mixture of inter- and intragranular fracture modes and a homogenous grain size distribution. The load–displacement behavior is linear for both temperatures and no unusual ferrous-elastic behavior was identified.

Acknowledgements

The authors would like to thank the CNPq and FINEP for their financial support.

References

[1] Y.P. Fu, H.C. Wang, Int. J. Hydrogen Energy 36 (2011) 747–754.
[2] K.J. Yoon, J.W. Stevenson, O.A. Marina, J. Power Sources 196 (2011) 8531–8538.
[3] J.W. Fergus, Solid State Ionics 171 (2004) 1–15.
[4] H. Yokokawa, N. Sakai, T. Horita, K. Yamaji, Fuel Cells 1 (2001) 117–131.
[5] T. Tiezt, Mater. Sci. Forum 426 (2003) 426–432.
[6] W.Z. Zhu, S.C. Deevi, Mater. Sci. Eng. A 348 (2003) 227–243.
[7] A. Chakraborry, R.N. Basu, H.S. Maiti, J. Mater. Lett. 45 (2000) 162–166.
[8] N. Sakai, H. Yokokawa, T. Horita, K. Yamaji, Int. J. Appl. Ceram. Technol. 1 (2003) 23–30.
[9] D.L. Maixer, R.A. Cutler, Solid State Ionics 146 (2002) 285–300.
[10] N.M. Sammes, R. Ratanaraj, J. Mater. Sci. 29 (1994) 4319–4324.
[11] L.F.G. Setz, I. Santacruz, M.T. Colomer, S.R.H. Mello-Castanho, R. Moreno, Mater. Res. Bull. 46 (2011) 983–986.
[12] N. Orlovskava, K. Kleveland, T. Grande, M.A. Einarsrud, J. Eur. Ceram. Soc. 20 (2000) 51–56.
[13] B.X. Huang, J. Malzbender, R.W. Steinbrech, E. Wessel, H.J. Penkalla, L. Singheiser, J. Membr. Sci. 349 (2010) 183–188.
[14] N.M. Sammes, R. Ratnaraj, J. Mater. Sci. 30 (1995) 4523–4526.
[15] S.H. Pi, S.B. Lee, R.H. Song, J.W. Lee, T.H. Lim, S.J. Park, D.R. Shin, C.O. Park, Int. J. Hydrogen Energy 36 (2011) 13735–13740.
[16] J.C. Rendón-Angeles, K. Yanagisawa, Z. Matamoros-Veloza, M.I. Pech-Canul, J. Mendez-Nonell, S.D. Torre, J. Alloys Compd. 504 (2010) 251–256.
[17] L.F.G. Setz, S.R.H. Mello-Castanho, R. Moreno, M.T. Colomer, Int. J. Appl. Ceram. Technol. 6 (2009) 626–635.
[18] J. Malzbender, R.W. Steinbrech, J. Power Sources 171 (2007) 60–67.